Journal of Computer-Aided Molecular Design, **16:** 167–179, 2002.
KLUWER/ESCOM

Investigation of the metal binding site in methionine aminopeptidase by density functional theory

Anne Techau Jørgensen[‡], Per-Ola Norrby[§] & Tommy Liljefors[‡,*]
[‡]*Department of Medicinal Chemistry, Royal Danish School of Pharmacy, Universitetsparken 2, DK-2100 Copenhagen, Denmark;* [§] *Technical University of Denmark, Department of Chemistry, Organic Chemistry, Building 201, Kemitorvet, DK-2800 Kgs. Lyngby, Denmark*

Received 20 March 2002; accepted 13 May 2002

Key words: angiogenesis, cobalt enzyme, density functional theory, hydroxide ion, methionine aminopeptidase, μ-hydroxo or μ-aquo bridge, zinc enzyme

Summary

All methionine aminopeptidases exhibit the same conserved metal binding site. The structure of this site with either Co^{2+} ions or Zn^{2+} ions was investigated using density functional theory. The calculations showed that the structure of the site was not influenced by the identity of the metal ions. This was the case for both of the systems studied; one based on the X-ray structure of the human methionine aminopeptidase type 2 (hMetAP-2) and the other based on the X-ray structure of the *E. coli* methionine aminopeptidase type 1 (eMetAP-1). Another important structural issue is the identity of the bridging oxygen, which is part of either a water molecule or a hydroxide ion. Within the site of hMetAP-2 the results strongly indicate that a hydroxide ion bridges the metal ions. By contrast, the nature of the oxygen bridging the metal ions within the metal binding site of eMetAP-1 cannot be determined based on the results here, due to the similar structural results obtained with a bridging water molecule and a bridging hydroxide ion.

Abbreviations: MetAP: Methionine aminopeptidase; eMetAP-1: *E. coli* methionine aminopeptidase type 1; hMetAP–2: human methionine aminopeptidase type 2.

Introduction

Angiogenesis is the name given to the formation of new blood vessels. It is an important process in the growth of tumours, and increases the rate of metastasis [1, 2]. Thus *anti*-angiogenic drugs are expected to inhibit tumour growth and decrease the likelihood of metastasis. It has been shown that inhibition of the enzyme methionine aminopeptidase type 2 blocks the proliferation of endothelial cells, and a correlation has been found between enzyme inhibition and anti-proliferative activity [3]. Furthermore, a potent angiogenesis inhibitor, fumagillin, inhibits methionine aminopeptidase binding to the active site [4, 5].

Methionine aminopeptidase occurs in two major isoforms in eukaryotes: type 1b and type 2b. By contrast, only type 1a occurs in eubacteria and archae only exhibit type 2a. All isoforms share the same overall fold, and the active sites of all sequenced MetAPs contain the same conserved metal binding site [6]. Three of the isoforms have been crystallographically characterised: *E. coli* MetAP type 1a (eMetAP-1) [7], human type 2b (hMetAP-2) [8], and *Pyrococcus furiosus* type 2a [9].

The conserved metal binding site is involved in the catalytic function of the protein and participates in the binding of some known inhibitors [10]. It consists of two metal ions bridged by either a water molecule or a hydroxide ion, and co-ordinated to two aspartates, two glutamates and one histidine (Figure 1). Experimental studies consistently indicate that the metal ions in the active site are cobalts; new data, however, sug-

*To whom correspondence should be addressed. E-mail: tl@dfh.dk

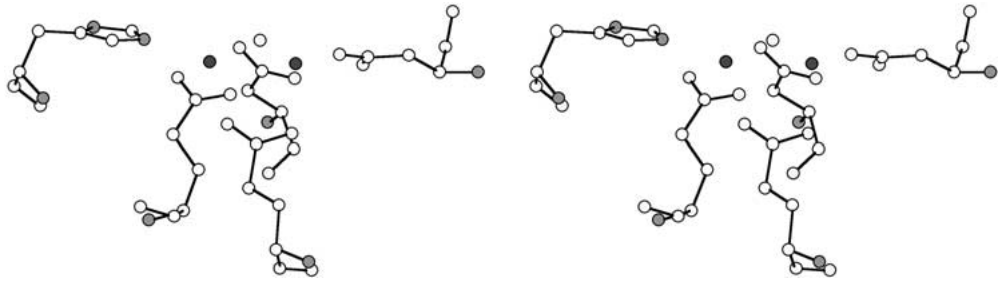

Figure 1. Stereoview of the metal ions (black atoms) and their ligands (D251, D262, H331, E364, E459, and the bridging oxygen) from the X-ray structure of hMetAP-2 (PDB code 1BOA).

gests that zinc is present *in vivo* in the case of yeast methionine aminopeptidase type 1 [11].

The nature of the bridging oxygen is not well established. Experimental data obtained by an electron paramagnetic resonance study on eMetAP-1 indicate that the bridging oxygen is part of a water molecule. The same study showed that 10–15% of the μ-oxo bridges is likely to be deprotonated to hydroxide anions at pH 9.65 [12].

In the present study we have investigated the structural issues discussed above, i.e. Co^{2+} *vs.* Zn^{2+} and H_2O *vs.* OH^- by density functional theory (DFT). Quantum chemistry presents a direct strategy for probing these questions. Calculations on the bimetal site of zinc-phosphotriesterase show that quantum chemical calculations on a model system give results in qualitative agreement with the molecular dynamics simulations; even though the surrounding protein environment is not taken into account [13]. Because several spin states are possible when the metal binding site includes two open shell Co^{2+} ions, the investigation also includes an evaluation of the possible spin state of the site containing Co^{2+} ions. The calculations serve to show whether the nature of the metals and bridging oxygen has any effect on the structure of the metal binding site.

Methods

Model systems for constrained geometry optimisations

Two model systems were constructed: one for the metal binding site of hMetAP-2 and one for that of eMetAP-1.

The model system for hMetAP-2 was based on the X-ray structure of hMetAP-2, co-crystallised with a ligand, fumagillin (PDB [14] code 1BOA). This X-ray structure was chosen over the one without ligand(PDB code 1BN5), because the latter does not include the important oxygen bridging the two metal ions. Test calculations on a system based on the X-ray structure without ligand indicate that the presence of the μ-oxo bridge is critical for reproducing the observed metal-metal distance even approximately (results not shown). Moreover, the heavy atom RMS deviation between the relevant atoms of the crystal structure with bridging oxygen *vs.* that without a determined bridging oxygen is as low as 0.132 Å, indicating that a bridging oxygen was present but was not detected.

Residues within 3.6 Å of the two metal ions were first extracted from the X-ray structure. This includes those parts of the five amino acids which co-ordinate to the metal ions, the two metal ions themselves, the bridging oxygen, and the hydroxy group of fumagillin. To model the site without ligand the hydroxy group of fumagillin is assumed to represent a free water molecule. The model was simplified by replacement of the aspartates and glutamates by formates, the histidine by an imidazole ring, and the hydroxy group by water (Figure 2a).

The model system for eMetAP-1 was based on the *E. coli* X-ray structure without ligand (PDB code 2MAT). The same procedure was used as for the model based on hMetAP-2. The extracted 3.6 Å sphere includes those parts of the five amino acids which co-ordinate to the metal ions, the two metal ions themselves, the bridging oxygen, a water molecule, and a threonine, which display hydrogen bonding to one of the glutamates. The model was simplified by replacement of the aspartates and glutamates by formates, the histidine by an imidazole ring, and the threonine by water (Figure 2b).

Additional calculations were performed on an eMetAP-1 model system to investigate the importance of the system size. Residues within 4.0 Å of the

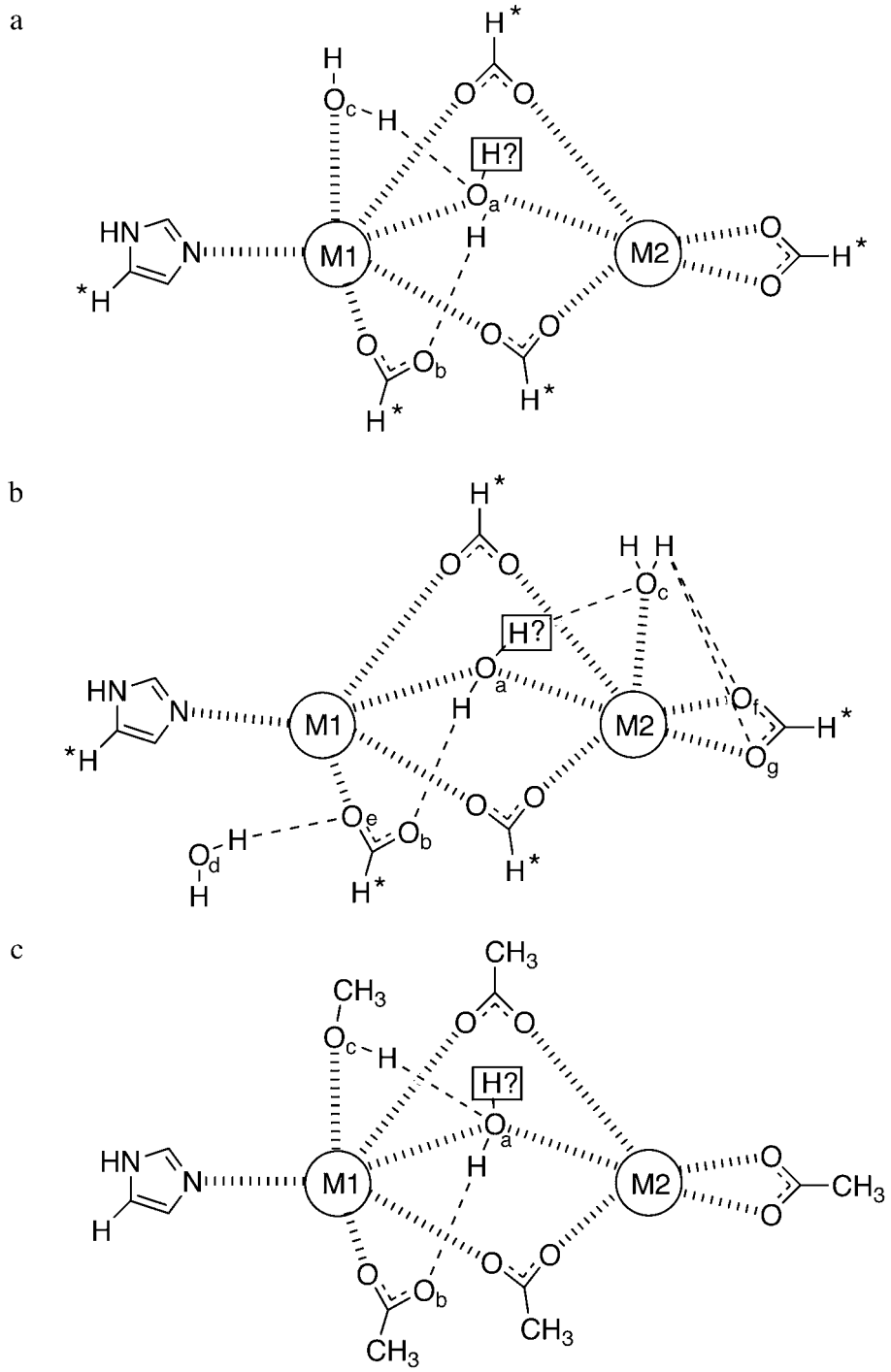

Figure 2. Schematic representation of the model systems used in this study. The oxygen bridging the two metal ions is either part of a water molecule or part of a hydroxide ion. a) The model system based on hMetAP-2 used for constrained geometry optimisations. The cartesian co-ordinates of the atoms marked with an asterisk were frozen. b) The model system based on eMetAP-1 used for constrained geometry optimisations. The cartesian co-ordinates of the atoms marked with an asterisk were frozen. c) The larger model system based on hMetAP-2 used for unconstrained geometry optimisations.

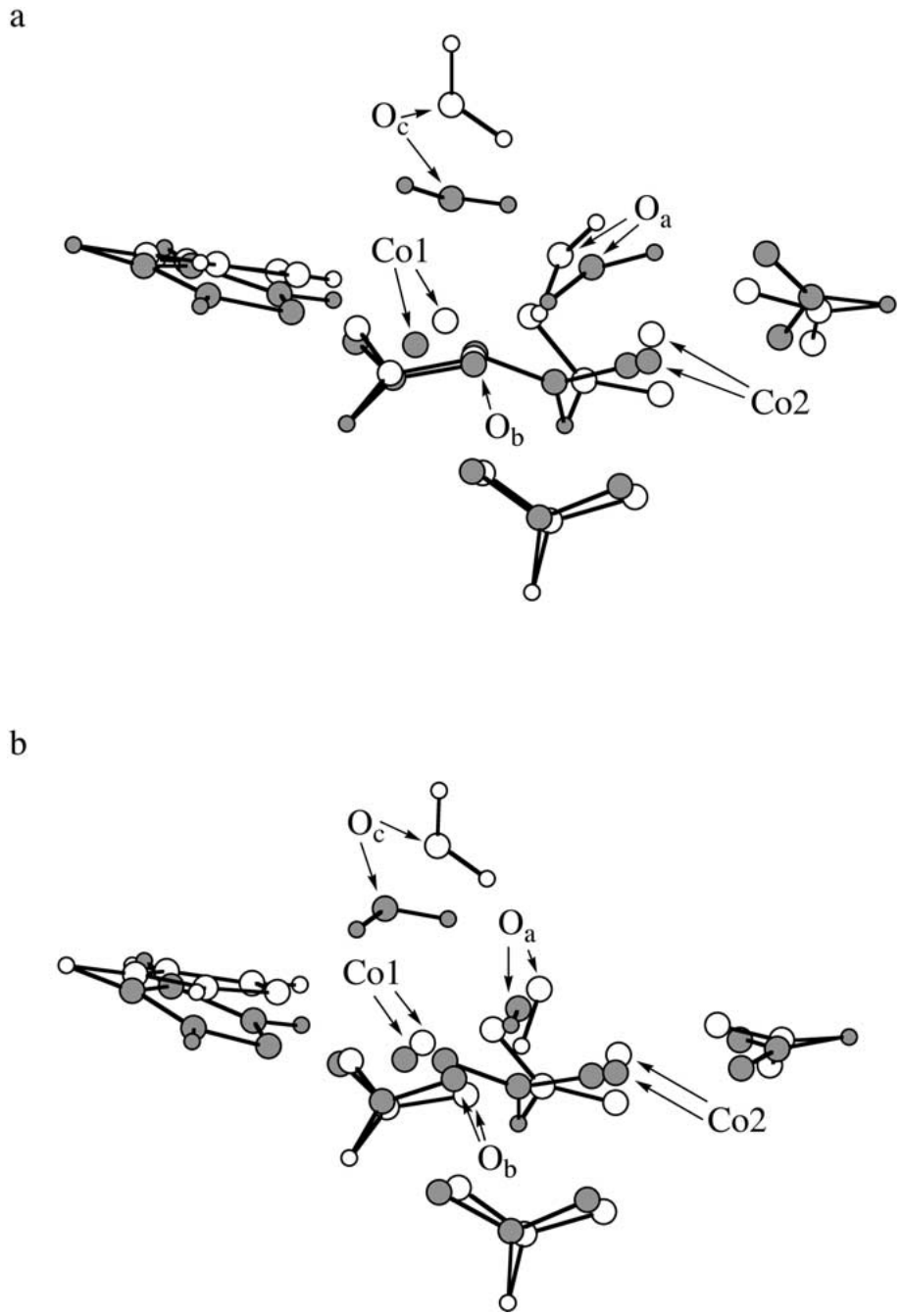

Figure 3. a) Superimposition of the converged structure of the constrained septet calculation on the model system for hMetAP-2 with cobalt and water (filled atoms) and the input structure. b) Superimposition of the converged structure of the constrained septet calculation on the model system for hMetAP-2 with cobalt and hydroxide ion (filled atoms) and the input structure. The hydrogens replacing the side chain carbons were used for the superimpositions.

Table 1. RMS deviation from the X-ray structure of the converged structures and relative energies of the converged wave functions calculated for the spin states of the cobalt-containing model for hMetAP-2.

Multiplicity – spin state[a]	spin of unpaired electrons Co1/Co2[b]	RMS (Å) H_2O[c]	RMS (Å) OH^-[d]	ΔE, kJ/mol[e] H_2O[c]	ΔE, kJ/mol[e] OH^-[d]
singlet – ll	α/β	0.630	NC[f]	132.5	NC[f]
singlet – hh	ααα/βββ	0.525	0.498	−0.5	−2.0
triplet – hl	ααα/β	0.539	0.399	80.1	79.9
triplet – ll	α/α	0.641	0.389	132.7	142.5
triplet – lh	α/βββ	0.661	0.496	42.3	62.0
quintet – hl	ααα/α	0.540	0.403	79.8	82.6
quintet – lh	α/ααα	0.662	0.495	42.7	64.0
septet – hh	ααα/ααα	0.527	0.496	0.0	0.0

[a]The S=1/2 spin state is denoted l and the S=3/2 spin state is denoted h. [b]See Figure 2 for atom labelling. [c]The bridging oxygen is part of a water molecule. [d]The bridging oxygen is part of a hydroxide ion. [e]The energies are relative to the energy of the corresponding septet. [f]Not calculated.

metal ions were extracted: the five amino acids which co-ordinate to the metal ions, the two metal ions themselves, the bridging oxygen, two additional waters and two threonines, both exhibiting a hydrogen bond to a metal ion co-ordinating carboxylate. The system was simplified in the same way as the 3.6 Å eMetAP-1 model system. Consequently, the model includes three extra waters compared to the 3.6 Å model, one of them being the simplified threonine. Because the converged structures of the septet calculations on this system (results not shown) were very similar to those of the smaller model system, the 3.6 Å model system was used for the calculations.

The Cartesian co-ordinates of the hydrogens replacing the side-chain carbons were frozen, in order to constrain the geometry optimisation of the model systems. Both model systems were tested with either a bridging water molecule (giving an overall neutral system) or a bridging hydroxide ion (giving a negatively charged complex). The distances in the X-ray structures indicate that one of the carboxylates could possibly form a hydrogen bond to the μ-oxo bridge. Thus, when transforming the bridging water molecule to a bridging hydroxide ion, the hydrogen-bonded proton was retained (Figure 2).

Model system for unconstrained geometry optimisation

A model was constructed based on the X-ray structure of hMetAP-2 (PDB code 1BOA). This model includes the same residues as those used for the constrained geometry optimisations described above. Because the geometries were not constrained during optimisation, better models of the residues were considered necessary and more carbons were included. Consequently, the model was simplified in the following way: the aspartates and glutamates were replaced by acetates; the histidine by an imidazole ring; and the fumagillin hydroxy group by methanol (Figure 2c).

Computational details

The model systems were constructed using MacroModel v. 7.0 [15]. In the model systems for constrained geometry optimisations hydrogens were added using Maestro v. 1.0. [16]. Hydrogens were added, and their positions were optimised using MMFF94 as implemented in Spartan v. 5.1.1. [17] to give an input structure for unconstrained geometry optimisations. All DFT calculations were performed *in vacuo* using Jaguar v. 4.0 [18] on SGI R10000 machines, with the B3LYP functional and the LACVP* basis set. B3LYP includes Becke's three-parameter hybrid exchange functional and the Lee-Yang-Parr correlation functional [19, 20]. LACVP is an effective core potential (ECP) basis set. Using this basis set the non-metal atoms are described by Pople's 6-31G basis set. Cobalt is described by the basis set optimised by Hay and Wadt [21] in a (331/311/41) contraction, where the 10 inner shell electrons are replaced by the ECP. Zinc is described by the basis set optimised by Hay and Wadt [22] in a (111/11/41) contraction, where the 18 inner shell electrons are replaced by the ECP. Unrestricted wave functions were used for all calculations including cobalts, whereas the zinc complexes

were calculated with a restricted wave function. Default settings were used with the following exceptions: the choice of loose geometry optimisation convergence criteria, and a maximum of 200 SCF iterations for each optimisation step. These adjustments were necessary due to slow SCF convergence for the metal complexes studied. To further improve convergence of the unconstrained calculations, the SCF level shift was set to 0.5-4. When convergence was reached, all calculations with higher SCF level shifts were further converged with a SCF level shift of 0.5. The level shift was set to 1 for the constrained geometry optimisation of the low spin/high spin quintet model for hMetAP-2. The geometry was subsequently reoptimised without level shift.

All possible combinations of low spin (S=1/2) and high spin (S=3/2) for each cobalt were tested in the constrained optimisations. The spin states of the cobalts were explicitly specified in the input files using the *atomic* and *bond* sections (A Jaguar input file is exemplified in Appendix). This procedure resulted in converged wave functions with the desired cobalt spin states. An exception was the low-spin singlet of the model system based on hMetAP-2. This calculation converged to a high-spin singlet.

Mulliken atomic spin densities were calculated for each optimised structure, in order to estimate the spin states of the cobalts according to the converged wave functions at the optimised geometries.

Results

Constrained geometry optimisations – model system based on hMetAP-2

The model of the metal binding site of hMetAP-2 with water and cobalt does not reproduce the co-ordination geometry found in the experimental structure, since the water molecule loses the co-ordination to one of the cobalts upon geometry optimisation. All calculations with a bridging water molecule and cobalt show one of the cobalts being ligated by the water molecule, while another water molecule approaches to co-ordinate to the other cobalt (Figure 3a). By contrast, the co-ordination pattern of the X-ray structure is reproduced, when an hydroxide ion bridges the two cobalts (Figure 3b). This finding is independent of the spin state of the system. The heavy atom RMS deviations from the crystal structure are generally lower for the cobalt calculations with bridging hydroxide than for those with bridging water (Table 1). The hMetAP-2-based model systems are most stable with both cobalts in high spin states; the high-spin singlet and septet are the most stable, independent of the bridge being part of a water molecule or a hydroxide ion. As a general trend, longer Co–Co distances were measured for the structures optimised with water (3.424 Å in the septet structure, Table 2) than for structures with hydroxide (3.244 Å in the septet structure, Table 2). For comparison the Co-Co distance of the experimental structure is 2.995 Å (Table 2). Large increases in Co-Co distances were found for the lower spin state calculations including water (Table 2). However, this is not the case for the higher spin states e.g. the septet, which display Co-Co distances within the probable experimental error.

Turning now to zinc, the calculations performed on the model for hMetAP-2 containing zinc ions gave results similar to those of the cobalt calculations. The water molecule does not bridge the two metal ions in the zinc optimised structure, and the co-ordination pattern resembles that of the septet calculation with cobalt and water. By contrast, the hydroxide ion does bridge the zinc ions, and the converged structure is thus similar to the structures optimised with cobalt and hydroxide ion.

Constrained geometry optimisations – model system based on eMetAP-1

The co-ordination geometries do not depend significantly on the identity of the metal ions, and the converged structures closely resemble the experimental structure (Figure 4). The heavy atom RMS deviations are low, independent on the nature of the μ-oxo bridge (Table 3). The most stable spin states are the high-spin singlet and septet, regardless of the identity of the bridging oxygen (Table 3). In the high-spin singlet state calculation with cobalt, the water molecule is found to transfer one of its hydrogens to one of the carboxylates, while still bridging the two cobalt ions. The distance between the oxygen of the water molecule and the transferred hydrogen is 1.519 Å, and the distance between this hydrogen and the carboxylate oxygen is 1.049 Å. Because the carboxylates are unstabilised due to the simplification of the model system, the hydrogen transfer is most likely a computational artefact. The structures optimised with water most often exhibit longer Co-Co distances (3.517 Å in the septet structure, Table 4) than those optimised with hydroxide ion (3.295 Å in the septet structure,

Table 2. Interatomic distances in the converged structures calculated for the spin states of the cobalt and zinc-containing models based on hMetAP-2.

Multiplicity	M1-M2 (Å)[b]		O_a-O_b (Å)[b]		O_a-O_c (Å)[b]		O_a-M1 (Å)[b]		O_a-M2 (Å)[b]	
– Spin state[a]	H_2O[c]	OH^-[d]	H_2O[c]	OH^-[d]	H_2O[c]	OH^-[d]	H_2O[c]	OH^-[d]	H_2O[c]	OH^-[d]
Experimental[e]	2.995	2.995	2.685	2.685	2.709	2.709	2.356	2.356	2.126	2.126
singlet – ll	3.820	NC[f]	2.581	NC[f]	2.665	NC[f]	3.409	NC[f]	2.169	NC[f]
singlet – hh	3.418	3.242	2.644	2.779	2.712	2.617	3.326	2.096	2.042	1.931
triplet – hl	3.767	3.377	2.627	2.831	2.734	2.632	3.210	2.066	2.208	1.915
triplet – ll	3.834	3.360	2.579	2.777	2.670	2.721	3.417	1.968	2.169	1.921
triplet – lh	3.531	3.247	2.612	2.743	2.696	2.688	3.569	1.998	2.026	1.944
quintet – hl	3.763	3.390	2.623	2.864	2.723	2.648	3.220	2.059	2.208	1.920
quintet – lh	3.549	3.262	2.610	2.736	2.693	2.680	3.586	2.002	2.025	1.948
septet – hh	3.424	3.244	2.641	2.796	2.707	2.605	3.331	2.115	2.043	1.935
Zinc	3.751	3.262	2.561	2.815	2.671	2.683	3.193	2.071	2.160	1.983
unconst. Co^{2+}[g]	3.409	3.135	2.567	2.758	2.700	2.740	3.004	2.003	2.047	1.980
unconst. Zn^{2+}[h]	3.641	3.195	2.585	2.785	2.630	2.700	3.177	2.020	2.077	2.009

[a]The S=1/2 spin state is denoted l and the S=3/2 spin state is denoted h. [b]See Figure 2 for atom labelling. [c]The bridging oxygen is part of a water molecule. [d]The bridging oxygen is part of a hydroxide ion. [e]From the X-ray structure of hMetAP-2 (PDB code 1BOA) containing Co^{2+}. [f]Not calculated. [g]From the unconstrained septet calculation with spin state: hh on the cobalt-containing model. [h]From the unconstrained calculation on the zinc-containing model.

Table 4). This trend was also present in the results generated with the model system based on hMetAP-2.

The structure optimised with zinc is similar to the structures optimised with cobalt, when a hydroxide ion is bridging the metal ions. The only significant difference with bridging water between the structures with cobalt and the structure with zinc lies with one of the co-ordinating carboxylates – the one that shows bidentate co-ordination to Co2 (Figure 5). This bidentate co-ordination is found in both the X-ray structure and in the structures with cobalt. Yet, the structure with zinc and water only exhibits monodentate co-ordination to Zn2. As a consequence of the altered co-ordination of the carboxylate, the heavy atom RMS deviation from the X-ray structure is as high as 0.448 Å (Table 5) for the structure derived with zinc and water.

Table 3. RMS deviation from the X-ray structure of the converged structures and relative energies of the converged wave functions calculated for the spin states of the cobalt-containing model for eMetAP-1.

Multiplicity – spin state[a]	RMS (Å) H_2O[b]	RMS (Å) OH^-[c]	ΔE, kJ/mol[d] H_2O[b]	ΔE, kJ/mol[d] OH^-[c]
singlet – ll	0.265	0.253	134.4	137.0
singlet – hh	0.242	0.169	43.9	36.6
triplet – hl	0.230	0.277	124.1	68.6
triplet – ll	0.262	0.290	132.2	133.3
triplet – lh	0.272	0.262	65.6	68.5
quintet – hl	0.235	0.298	121.8	67.4
quintet – lh	0.292	0.260	35.9	70.1
septet – hh	0.261	0.222	0.0	0.0

[a]The S=1/2 spin state is denoted l and the S=3/2 spin state is denoted h. [b]The bridging oxygen is part of a water molecule. [c]The bridging oxygen is part of a hydroxide ion. [d]The energies are relative to the energy of the corresponding septet.

Unconstrained geometry optimisations including cobalt and water

In the experimental structure of hMetAP-2, both of the cobalt atoms display a distorted square pyramidal co-ordination geometry. This type of co-ordination geometry is reproduced by singlet- and triplet state calculations of the model system, when cobalt and water are included. This is not the case for the quintet and the septet calculations, which display a different type of cobalt co-ordination. One of the cobalt ions exhibits square pyramidal co-ordination, though in a orientation different from that found in the X-ray structure, while the other cobalt is present in a tetrahedral arrangement exhibiting monodentate co-ordination as that of the eMetAP-1 structure including zinc and water (Figure 6). The septet (high-spin/high-spin) is the most stable spin state when a water molecule is bridging. Notably, the central water does not bridge the cobalts, according to the triplet, quintet and septet op-

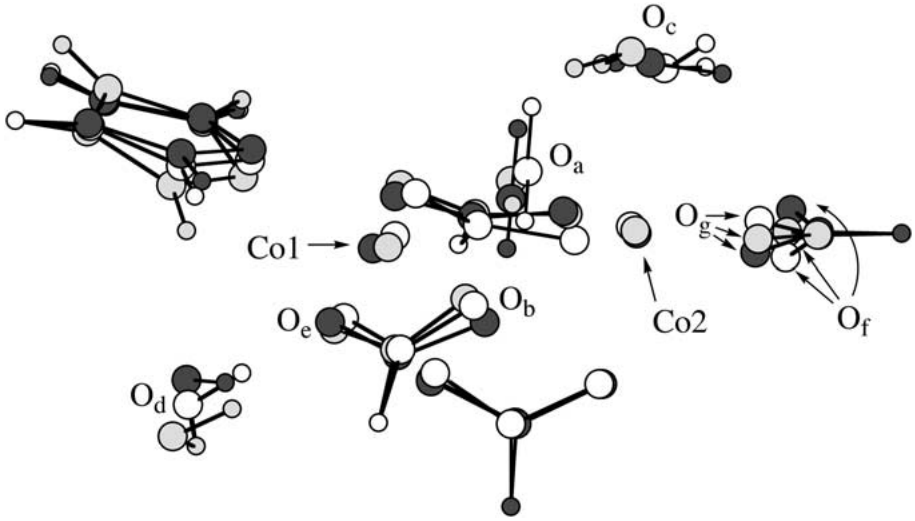

Figure 4. Superimposition of the converged cobalt/water structure of the constrained septet calculation on the model system for eMetAP-1 (filled atoms), the converged cobalt/hydroxide structure of the same system (light grey atoms) and the input structure (white atoms). The hydrogens replacing the side chain carbons were used for the superimposition. The cobalt/water and the cobalt/hydroxide structures are very similar, and both structures resemble the experimentally determined one.

timisations; instead the hydroxy group becomes the fifth ligand for one of the cobalts. Thus instead of a single bridging oxygen, each cobalt co-ordinates to a separate oxygen (from the hydroxy group or water). In the singlet state, the water oxygen partly transfer one of its hydrogens to one of the carboxylates, while still bridging the two cobalt ions. The distance between the water oxygen and the proton is 1.190 Å, and the distance between the proton and the carboxylate oxygen is 1.233 Å. As was the case in the constrained calculation, the hydrogen transfer is likely an artefact introduced by the simplification of the model system. Even though the geometries optimised with water bridging are qualitatively different from the X-ray structure, the heavy atom RMS deviations are reasonably low, 0.772-1.071 Å.

Unconstrained geometry optimisations including cobalt and hydroxide

The geometries obtained from optimisation of the model system including cobalt and hydroxide vary little, regardless of the spin state specified. All converged geometries exhibit distorted square pyramidal co-ordination around the two cobalts, and the same hydrogen-bonding pattern. This common geometry qualitatively reproduces the experimental structure. The septet is again the most stable spin state, and of the geometries including cobalt and hydroxide ion, this one exhibits the lowest heavy atom RMS-deviation from the crystal structure, 0.870 Å (Table 5). For all spin states, the cobalt–cobalt distance is shorter with hydroxide than with water bridging. The distance is 3.409 Å within the converged structure of the septet calculation with water bridging and 3.135 Å with hydroxide ion bridging (Table 2).

Unconstrained geometry optimisations including zinc

The co-ordination numbers of the two zinc ions vary, depending on the nature of the bridging oxygen. With hydroxide, both zinc ions manifest as distorted square pyramids. Another co-ordination geometry is found with water. One zinc ion displays a distorted square pyramidal geometry, in an orientation different from that of the X-ray structure, while the other has tetrahedral geometry. Thus, the results of the zinc and water optimisations are very similar to those of the quintet and septet calculations including cobalt and water (Figure 6). In exactly the same fashion, one of the zincs has picked up a new fifth ligand, via the hydroxy oxygen. Even though the structure optimised with zinc and water differs qualitatively from the experimental structure, the RMS deviation between the two is comparable to that of the structure optimised with zinc and hydroxide 0.789 Å with water and 0.784 Å with hydroxide (Table 5). As was the case for the cobalt calculations, the zinc–zinc distance is longer with water bridging (3.641 Å, Table 2) than with hydroxide bridging (3.195 Å, Table 2).

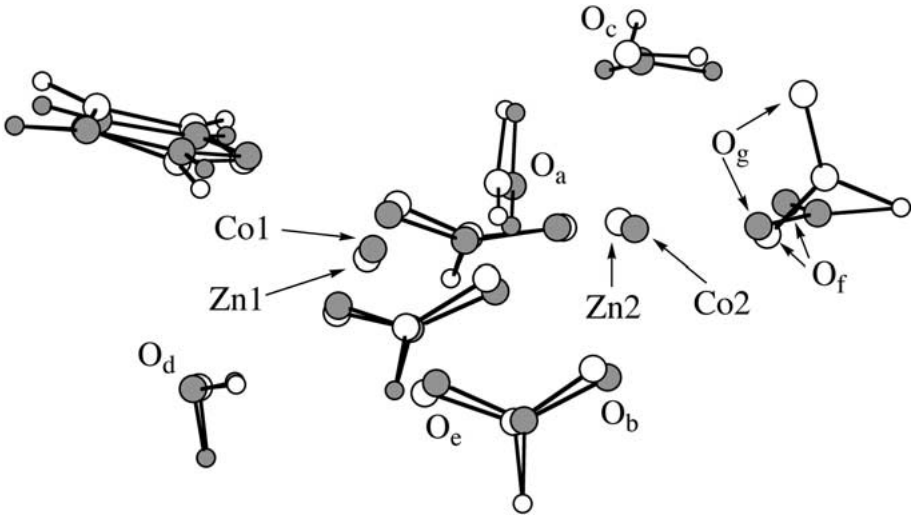

Figure 5. Superimposition of the structure of the constrained septet calculation on the model system based on eMetAP-1 with cobalt and water (filled atoms) and the structure of the same model system with zinc and water. The hydrogens replacing the side chain carbons were used for the superimposition. The only major structural difference is the mono- vs. bidentate co-ordination of the carboxylate.

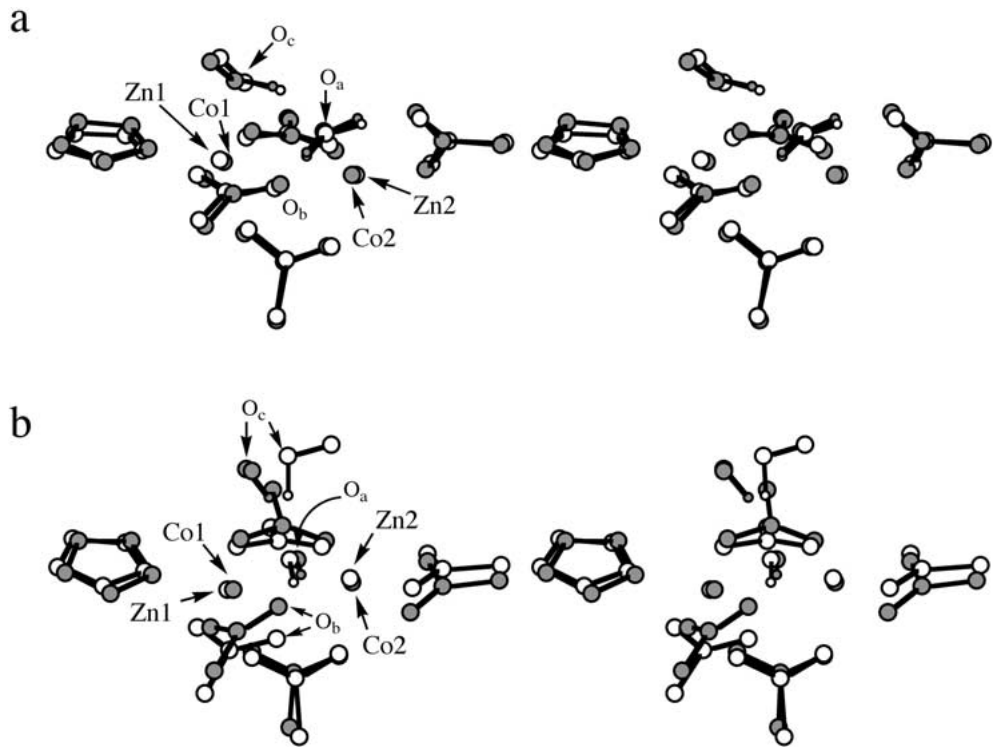

Figure 6. Superimpositions of the converged structures of the unconstrained septet calculations with cobalt and the structures of the unconstrained calculations with zinc. Only hydrogens potentially participation in hydrogen bonds are shown for clarity. a) Superimposition of the structure with cobalt and water (filled atoms) and the structure with zinc and water. b) Superimposition of the structure with cobalt and hydroxide (filled atoms) and the structure with zinc and hydroxide.

Table 4. Interatomic distances in the converged structures calculated for the spin states of the cobalt and zinc-containing models based on eMetAP-1.

Multiplicity	M1-M2 (Å)[b]		O_a-O_b (Å)[b]		O_a-O_c (Å)[b]		O_d-O_e (Å)[b]		O_c-O_f (Å)[b]		O_c-O_g (Å)[b]	
– Spin state[a]	H_2O[c]	OH^-[d]	H_2O[c]	OH^-[d]	H_2O[c]	OH^-[d]	H_2O[c]	OH^-[d]	H_2O[c]	OH^-[d]	H_2O[c]	OH^-[d]
Experimental[e]	3.174	3.174	2.856	2.856	2.985	2.985	2.771	2.771	2.968	2.968	3.251	3.251
singlet – ll	3.677	3.356	2.546	2.780	2.940	2.728	2.794	2.859	3.019	3.078	2.729	3.285
singlet – hh	3.348	3.269	2.553	2.810	2.890	2.790	3.061	2.929	3.137	3.349	2.634	3.227
triplet – hl	3.554	3.222	2.466	2.717	3.098	2.769	2.844	2.866	3.034	2.902	2.689	3.204
triplet – ll	3.672	3.350	2.548	2.776	2.940	2.727	2.794	2.839	2.848	3.004	2.844	3.272
triplet – lh	3.700	3.347	2.513	2.817	2.805	3.116	2.752	2.874	2.822	3.164	3.178	3.529
quintet – hl	3.527	3.256	2.461	2.736	3.262	2.767	2.839	2.833	3.097	2.910	2.642	3.174
quintet – lh	3.661	3.353	2.511	2.821	2.860	2.808	2.749	2.869	2.691	3.168	3.264	3.476
septet – hh	3.517	3.295	2.457	2.869	2.815	2.766	2.843	2.907	2.697	3.178	3.337	3.448
Zinc	3.415	3.252	2.465	2.849	2.653	2.633	2.716	2.909	3.020	3.409	2.570	3.453

[a]The S=1/2 spin state is denoted l and the S=3/2 spin state is denoted h. [b]See Figure 2 for atom labelling. [c]The bridging oxygen is part of a water molecule. [d]The bridging oxygen is part of a hydroxide ion. [e]From the X-ray structure of eMetAP-1 (PDB code 2MAT) containing Co^{2+}.

Discussion

The available experimental structures of MetAP's include cobalt ions as the metal ions in the active site. The identity of the metal ions *in vivo* is still under debate. Our results reveal that the identity of the metal ions is of minor importance for the structure of the site. As expected, the calculated geometry depends on whether constrained or unconstrained optimisations are performed, and whether the model system is based on the experimental structure of hMetAP-2 or eMetAP-1. Nevertheless, within each pair of results, cobalt and zinc lead to similar structures. The constrained and unconstrained calculations give similar results for the metal co-ordination sphere, even though the position of the anchor points (methyl groups or hydrogens) are rather different. The nature of the bridging oxygen seems to be more important, at least for the model system based on hMetAP-2. In this case, the hydroxide ion bridges the two metal ions; by contrast, the water molecule only co-ordinates to one of the cobalts and hence the structure does *not* resemble the experimental structure. This is a good indication that the bridging oxygen is actually part of an hydroxide ion within the active site of hMetAP-2. Moreover, the cobalt–cobalt distances found with hydroxide are comparable to that of the X-ray structure, while significantly longer cobalt–cobalt distances result when water is bridging, both in the constrained and the unconstrained calculations. This finding is consistent with comparable theoretical calculations on zinc-phospotriesterase. Using both molecular dynamics and quantum chemical calculations Zhan *et al*. [13] find a longer zinc-zinc distance with a μ-aquo bridge than with a μ-hydroxo bridge. With water the distance is 4.195 Å and with hydroxide the distance is 3.353 Å using B3LYP/6-31G* [13].

The results of the calculations for the eMetAP-1-based model system are less clear-cut. The experimental structure is well reproduced independent of the nature of the oxygen bridging the cobalts. The heavy atom RMS deviations from the crystal structure are generally low, both when water is bridging and when hydroxide is bridging, and no important structural differences are found. Thus, the results cannot be used to conclude the nature of the bridging oxygen – a water molecule or a hydroxide ion could equally well be bridging the metal ions. One explanation for the stability of a water-bridge in the eMetAP-1 site, while its presence is unlikely in the case of hMetAP-2, is that E204 (E364 in hMetAP-2) of eMetAP-1 gains additional stabilisation from hydrogen bond donation by T202 – the corresponding residue in hMetAP-2 is an alanine.

The constrained systems are most stable when both cobalts exhibit high-spin states; this is the case for both model systems with water as well as hydroxide. These theoretical findings are in reasonable agreement with experimental data obtained by an electron paramagnetic resonance study on eMetAP-1. D'souza *et al.* [12] report an $S = 3/2$ ground state, exhibiting no significant spin–spin interaction at pH 7.5. At pH

Table 5. RMS deviation from the X-ray structure of the converged structures calculated for the zinc-containing models of hMetAP-2 and eMetAP-1 and that of the septet unconstrained calculation on the model of hMetAP-2.

c/u – model – M^{2+a}	RMS (Å) H_2O^b	RMS (Å) OH^{-c}
c – hMetAP-2 – Zn	0.560	0.463
c – eMetAP-1 – Zn	0.448	0.213
u – hMetAP-2 – Zn	0.789	0.784
u – hMetAP-2 – Co	0.772	0.870

[a]Constrained calculations are marked c, unconstrained u. [b]The bridging oxygen is part of a water molecule. [c]The bridging oxygen is part of a hydroxide ion.

9.65, however, an additional population, ∼5-15% is found, in which the two cobalts are ferromagnetically coupled, possibly leading to an $S = 3$ ground state. It is suggested that this additional population is due to deprotonation of the bridging water [12]. A shorter Co–Co distance is found in calculations with bridging hydroxide, and the shorter distance increases the probability of spin coupling. Assuming the two cobalts do not exhibit spin–spin coupling, both the high-spin singlet and septet states treated here are in accordance with the experimental data.

Conclusions

The calculations have shown that the structure of the investigated metal binding site is not influenced by the identity of the metal ions (Co^{2+} or Zn^{2+}). In the model system based on the crystal structure of hMetAP-2, the optimisations with zinc or cobalt present lead to very similar geometries. The same is the case with the models based on eMetAP-1. Moreover, the unconstrained optimisations generally give zinc-containing geometries resembling the cobalt-containing geometries. Since the calculations with water do not reproduce the experimental structure, the results strongly indicate that a hydroxide ion is bridging the metal ions within the active site of hMetAP-2. By contrast, the nature of the oxygen bridging the metal ions within the metal binding site of eMetAP-1 cannot be determined based on the results here, due to the similar structural results obtained with a bridging water molecule and a bridging hydroxide ion.

Acknowledgements

This work was financially supported by Graduate School of Drug Research and LEO-Pharma, which are gratefully acknowledged.

References

1. Folkman, J., Nat. Med., 1 (1995) 27.
2. Folkman, J., N. Eng. J. Med., 333 (1995) 1757.
3. Griffith, E.C., Su, Z., Turk, B.E., Chen, S., Chang, Y.-H., Wu, Z., Biemann, K. and Liu, J.O., Chem. Biol., 4 (1997) 461.
4. Lowther, W.T., McMillen, D.A., Orville, A.M. and Matthews, B.W., Proc. Natl. Acad. Sci. USA, 95 (1998) 12153.
5. Griffith, E.C., Su, Z., Niwayama, S., Ramsay, C.A., Chang, Y.-H. and Liu, J.O., Proc. Natl. Acad. Sci. USA, 95 (1998) 15183.
6. Bradshaw, R.A., Brickey, W.W. and Walker, K.W., Trends Biochem. Sci., 23 (1998) 263.
7. Lowther, W.T., Orville, A.M., Madden, D.T., Lim, S., Rich, D.H. and Matthews, B.W., Biochemistry, 38 (1999) 7678.
8. Liu, S., Widom, J., Kemp, C.W., Crews, C.M. and Clardy, J., Science, 282 (1998) 1324.
9. Tahirov, T.H., Oki, H., Tsukihara, T., Ogasahara, K., Yutani, K., Ogata, K., Izu, Y., Tsunasawa, S. and Kato, I., J. Mol. Biol., 284 (1998) 101.
10. Lowther, W.T., Zhang, Y., Sampson, P.B., Honek, J.F. and Matthews, B.W., Biochemistry Usa, 38 (1999) 14810.
11. Walker, K.W. and Bradshaw, R.A., Protein Sci., 7 (1998) 2684.
12. D'souza, V.M., Bennett, B., Copik, A.J. and Holz, R.C., Biochemistry, 39 (2000) 3817.
13. Zhan, C.-G., de Souza, O.N., Rittenhouse, R. and Ornstein, R.L., J. Am. Chem. Soc., 121 (1999) 7279.
14. Berman, H.M., Westbrook, J., Feng, Z., Gilliland, G., Bhat, T.N., Weissig, H., Shindyalov, I.N. and Bourne, P.E., Nucl. Acids. Res., 28 (2000) 235.
15. Mohamadi, F., Richards, N.G.J., Guida, W.C., Liskamp, R., Lipton, M., Caufield, C., Chang, G., Hendrickson, T. and Still, W.C., J. Comput. Chem., 11 (1990) 440.
16. Maestro, Schrödinger, Inc., Portland, OR, 1999-2000.
17. Spartan 5.1.1, Wavefunction, Inc., Irvine, CA, 1991-1998.
18. Jaguar 4.0, Schrödinger, Inc., Portland, OR, 1991-2000.
19. Becke, A.D., J. Chem. Phys., 98 (1993) 5648.
20. Lee, C., Yang, W. and Parr, R.G., Phys. Rev. B, 37 (1988) 785.
21. Hay, P.J. and Wadt, W.R., J. Chem. Phys., 82 (1985) 299.
22. Hay, P.J. and Wadt, W.R., J. Chem. Phys., 82 (1985) 270.

Appendix

The jaguar input file used in the high spin singlet geometry optimisation of the model system for hMetAP-2 with H_2O.

This JAGUAR input file generated by Babel 1.3
&gen
iaccg=3
idft=22111
igeopt=1
iguess=25
iuhf=1
maxit=200
multip=1
basis=LACVP*
ip11=2
&
&zmat

H1	0.0000000000000#	0.0000000000000#	0.0000000000000#
C2	0.0000000000000	0.0000000000000	11.0903348945100
C3	0.2427759894519	0.0000000000000	1.0664660921480
O4	1.3774032369904	−0.3873504810534	1.4293792001920
O5	−0.5783834693880	0.4460156464647	1.9068082595251
H6	3.8164603391752#	−0.6835278601926#	5.5939454966372#
C7	2.8064270064434	−0.6911570780871	5.1462365426168
O8	2.6867937272198	−0.4149197787846	3.9274943668567
O9	1.8164774445565	−0.9507159867316	5.8535530346227
N10	1.0307903991968	−0.8922947001676	10.8729093371841
C11	−0.4126783304335	0.4709740054685	9.8727473798840
C12	1.2282151788773	−0.9634578650939	9.5682928186909
N13	0.3873054328459	−0.1704078826046	8.9500819984175
H14	−1.2036594835802#	4.1444685481987#	6.9019137065776#
C15	−1.2483937774296	3.1083612454197	6.5026582388945
O16	−1.4701393000406	2.9198183121390	5.2750563142009
O17	−1.0750595855854	2.1449801824982	7.2567462334571
H18	2.6421880017347#	3.6764204344552#	4.8546419960374#
C19	2.1908357506987	2.6614308944336	4.7568071672778
O20	2.1484822356885	2.1434563584925	3.6079480567308
O21	1.8127417940485	2.1780973325585	5.8247836416956
H22	−3.4014024338153	−1.3932862717477	6.3239385257608
O23	−2.4748015425869	−1.0578023254011	6.3865477969464
Co24	0.3821429143696	0.5539865391105	6.5635210890305
Co25	0.8937465719427	0.0616794962171	3.6539583581265

```
O26    −0.9653711646971      0.3603677288511      4.6406504919764
H27    −2.2058975885573     −0.6988876238561      5.5377438462186
H28    −1.2131499385156      1.1937948300318      9.8164176666112
H29     1.9379859236529     −1.5463489973251      9.0000823500941
H30    −0.3324639775633#     0.2061375169686#    12.0970004002298#
H31     1.6076466382687     −1.3916452619148     11.5347150024025
H32    −1.6789014637382      0.3165220539964      3.9999072657174
H33    −0.7109268419399      1.2762689068798      4.7747527483043
&
&atomic
atom formal multip
Co24    2    4
Co25    2    4
O4     −1    1
O9     −1    1
O20    −1    1
O17    −1    1
&
&bond
atom alpha beta
Co24    3    0
Co25    0    3
&
```